UNSTEADY HOMOGENEOUS-HETEROGENEOUS REACTIONS IN MHD NANOFLUID MIXED CONVECTION FLOW PAST A STAGNATION POINT OF AN IMPULSIVELY ROTATING SPHERE

by

Abd El Nasser MAHDY[a*], Fekry M. HADY[b], and Hossam A. NABWEY[c,d]

[a] Faculty of Science, South Valley University, Qena, Egypt
[b] Faculty of Science, Assiut University, Assiut, Egypt
[c] College of Science and Humanities, Prince Sattam bin Abdulaziz University, Al-Kharj, Saudi Arabia
[d] Faculty of Engineering, Menoufia University, Shebin El-Kom, Egypt

Original scientific paper
https://doi.org/10.2298/TSCI190712388M

This paper establishes a mathematical analysis for describing the homogeneous and heterogeneous chemical reactions in the nearness of stagnation region of a sphere immersed in a single-phase nanofluid due to a Newtonian heating. The flow is resulted by an impulsively rotating sphere, and the nanofluid involves nanoparticles of copper and ferro. The available unsteady-states of the considered system are given in the case when the diffusion coefficients of both reactant and auto catalyst have the same size. The resulting non-linear dimensionless coupled PDE in which governing the mixed convection flow have been tackled numerically via an implicit finite difference technique in combination with the quasi-linearization scheme. The similarities and differences in the behavior of physical pertinent fluid parameters have been elaborated and discussed graphically. It has been clarified that the nanofluid velocity and temperature profiles grow gradually by adding nanoparticles in the base fluid. Again it is noticed from present contribution that concentration of the nanofluid is decreases function by rising the strength of homogeneous and heterogeneous chemical reactions. Finally, numerical computations of the skin friction and heat transfer factors are presented.

Key words: *single-phase nanofluid, unsteady mixed, convective condition, homogeneous-heterogeneous reactions, sphere, heat generation*

Introduction

Varied systems of chemically reacting arise through both heterogeneous and homogeneous reactions with instances arising in catalysis, combustion and biochemical systems. The relationship between heterogeneous reactions arising on some catalytic surfaces and homogenous reactions in the bulk of fluid is often particularly convoluted, including the production and consumption of reactant species at non-similar rates both on the catalytic surface and inside the fluid. Besides the feedback on these reaction rates through fluid temperature variations inside the reacting fluid, which leads to change the fluid motion. Therefore there exists a three-way coupling between fluid, fluid-surface temperatures, and reactant species concentrations. A number of catalyst-driven reactions, which are of significance in the chemical

* Corresponding author, e-mail: mahdy@svu.edu.eg

process, there can be a cognizable reaction within the bulk (homogeneous reactions) and on the catalyst surface. Song *et al.* [1-3] and Williams *et al.* [4, 5] presented some examples of such homogeneous and heterogeneous reactions. Additionally, Chaudhary and Merkin [6, 7] have been presented a simple model for homogeneous and heterogeneous reactions in boundary-layer flow in which the heterogeneous (surface) reaction is considered to be raised by first order kinetics while homogeneous (bulk) reaction by isothermal cubic autocatalator kinetics. They have investigated the possible steady-states of their model in the particularly case when the diffusion coefficients of both reactant and autocatalyst are of the same size. Moreover, Merkin [8] has exhibited the boundary-layer flow of a uniform stream along a flat surface (Blasius solution) employing the same model of homogeneous and heterogeneous reaction. Hayat *et al.* [9] scrutinized simulation and modeling for chemically reacting Maxwell liquid according to modified Fourier approach. Khan and Pop [10] modeled the homogeneous and heterogeneous situation of reactions in viscoelastic fluid flow by stretching plate. Khan *et al.* [11] and Hayat *et al.* [12] disclosed homogeneous and heterogeneous reactions for viscous nanofluid and Maxwell fluid flow through slender surface.

Due to the low thermal conductivity of some fluids like water, oil, and ethylene glycol mixtures, the convectional heat transfer of these fluids are poor. The fluid thermal conductivity may be enhanced by hanging nano-sized particle materials in the liquid to arise a nanofluid. Nanofluid is a developed kind of material involving suspension of solid particles so-called nanoparticles. Nanofluid flow and heat transfer along a stretchable cylinder with applying magnetic field has been exhibited by Ashorynejad *et al.* [13]. They elaborated that choosing copper (for small of magnetic parameter) and alumina (for large values of magnetic parameter) results in the highest cooling performance. Abu-Nada *et al.* [14] reported free convection heat transfer improvement in horizontal concentric annuli field by nanofluid. Tiwari and Das [15] modified a model to describe the behavior of nanofluids considering the solid volume fraction. A number of extensive contributions of nanofluids and therein can be found in [16-32].

Besides, due to their applications in industry and engineering, the investigation of steady and unsteady uniform fluid flows on rotating sphere in which its axis of rotation parallel to the ambient velocity has been recognized by many researchers applying several analytical and numerical methods [33-36]. Motivated by such facts, this paper inspects the combined impacts of a homogeneous and heterogeneous reactions subject to internal heat generation in MHD mixed convection nanofluid flow around an impulsively rotating sphere. This investigation allowed to use the model developed by Merkin [8] for homogeneous and heterogeneous reactions in boundary-layer flow with cubic autocatalysis. The non-dimensional transformed boundary-layer equations of motion and concentration have been tackled numerically. To our best knowldge, this specific problem hasn't been addressed before. Special cases of the current results are compared with those of Takhar *et al.* [34].

Flow configuration

Let us inspect an unsteady, 2-D, incompressible, boundary-layer nanofluid flow of MHD mixed convection in stagnation of an impulsively rotating sphere with existence of heat generation or absorption impact. A single-phase model is applied to simulate the nanofluid flow. The sphere rotates with a constant angular velocity, Ω, around a diameter parallel to the ambient free stream velocity $U(x) = \tilde{a}x$, as depicted in fig. 1. Besides, an external constant uniform magnetic field with strength, B_0, is given in z-direction. Before time $t = 0$, the sphere is at rest in an ambient fluid and surface temperature equals T_∞. The fluid has constant physical properties with excluding the density which reults the buoyancy force. The impacts of viscous

dissipation and Joul heating is considered to be absent. Furthermore, a simple homogeneous-heterogeneous reaction model is assumed as given by Chaudhary and Merkin [25] and Merkin [8] as:

$$A + 2B \to 3B, \quad \text{rate} = k_c ab^2 \tag{1}$$

but on the catalyst surface single, isothermal, first order chemical reaction *i. e.* heterogeneous, is given:

$$A \to B, \quad \text{rate} = k_s a \tag{2}$$

in which a and b point out concentrations of the chemical species, A and B, k_c, and k_s symbolize the rate constants. It is supposed that both reaction processes are isothermal. Follow these assumptions, the boundary-layer equations that depicting nanofluid flow can be stated in dimensional form as [25, 28];

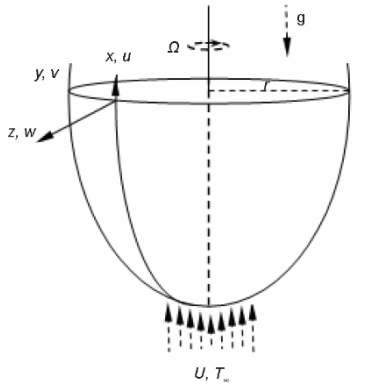

Figure 1. Flow model and co-ordinate system

$$\frac{\partial (xu)}{\partial x} + \frac{\partial (xw)}{\partial z} = 0 \tag{3}$$

$$\rho_{\text{nf}} \left(\frac{\partial u}{\partial t} + u\frac{\partial u}{\partial x} + w\frac{\partial u}{\partial z} - \frac{v^2}{x} \right) = \rho_{\text{nf}} U \frac{\partial U}{\partial x} + \mu_{\text{nf}} \frac{\partial^2 u}{\partial z^2} - \sigma_{\text{nf}} B_0^2 (u - U) + \frac{gx}{r} (\rho\beta)_{\text{nf}} (T - T_\infty) \tag{4}$$

$$\rho_{\text{nf}} \left(\frac{\partial v}{\partial t} + u\frac{\partial v}{\partial x} + w\frac{\partial v}{\partial z} + \frac{uv}{x} \right) = \mu_{\text{nf}} \frac{\partial^2 v}{\partial z^2} - \sigma_{\text{nf}} B_0^2 v \tag{5}$$

$$(\rho c_p)_{\text{nf}} \left(\frac{\partial T}{\partial t} + u\frac{\partial T}{\partial x} + w\frac{\partial T}{\partial z} \right) = k_{\text{nf}} \frac{\partial^2 T}{\partial z^2} + Q_0 (T - T_\infty) \tag{6}$$

$$\frac{\partial a}{\partial t} + u\frac{\partial a}{\partial x} + w\frac{\partial a}{\partial z} = D_A \frac{\partial^2 a}{\partial z^2} - k_c ab^2 \tag{7}$$

$$\frac{\partial b}{\partial t} + u\frac{\partial b}{\partial x} + w\frac{\partial b}{\partial z} = D_B \frac{\partial^2 b}{\partial z^2} + k_c ab^2 \tag{8}$$

The recognized boundary conditions for flow governing eqs. (3)-(8) are taken as:

$$\text{At}: \quad z = 0, \quad u(t,x) = w(t,x) = 0, \quad v(t,x) = \Omega x, \quad k_{\text{f}} \frac{\partial T}{\partial z} = h_{\text{f}} (T - T_{\text{f}})$$

$$D_A \frac{\partial a}{\partial z} = k_s a, \quad D_B \frac{\partial b}{\partial z} = -k_s a$$

$$\text{As}: \quad z \to \infty, \quad u \to U, \quad v \to 0, \quad T \to T_\infty, \quad a \to a_0, \quad b \to 0 \tag{9}$$

Notations u, v, and w explain the nanofluid velocity components in the x-, y-, and z-directions, respectively, μ_{nf} gives the dynamic viscosity of the nanofluid, density of the

nanofluid is given by ρ_{nf}, σ_{nf} represents electrical conductivity of the nanofluid, T means the temperature of the nanofluid, Q_0 refers to the internal heat generation or absorption coefficient, D_A and D_B indicate the respective diffusion coefficients, T_∞ is the nanofluid temperature of free stream, and h_f indictates the convective heat transfer.

Brinkman [37] presented the dynamic viscosity of the nanofluid:

$$\mu_{nf} = \mu_f (1-\varphi)^{-5/2} \tag{10}$$

in which the solid volume fraction of nanoparticles is indicated by φ. The effective density of the nanofluid, ρ_{nf}, and the nanofluid thermal expansion coefficient, β_{nf}, are approximated [15]:

$$\rho_{nf} = (1-\varphi)\rho_f + \varphi\rho_p \tag{11}$$

$$\beta_{nf} = (1-\varphi)\beta_f + \varphi\beta_p \tag{12}$$

where $(\rho c_p)_{nf}$ indicates the heat capacitance of the nanofluid and is defined [15]:

$$(\rho c_p)_{nf} = (1-\varphi)(\rho c_p)_f + \varphi(\rho c_p)_p \tag{13}$$

Furthermore, k_{nf} points out thermal conductivity of the nanofluid, due to Maxwell-Garnetts (MG) model [38] it is approximated:

$$k_{nf} = k_f \frac{k_p + 2k_f + 2\varphi(k_p - k_f)}{k_p + 2k_f - \varphi(k_p - k_f)} \tag{14}$$

Finally, the nanofluid effective electrical conductivity is approximated [38]:

$$\sigma_{nf} = \sigma_f \left[1 + \frac{3(\sigma-1)\varphi}{(\sigma+2) - (\sigma-1)\varphi}\right], \quad \left(\sigma = \frac{\sigma_p}{\sigma_f}\right) \tag{15}$$

Notice the subscripts, nf, explains the nanofluid thermophysical properties, f, refers to base fluid, but, p, is known as nano-solid particles. Table 1 stands for the thermophysical values of the nanofluids given in this investigation.

Table 1. Thermophysical properties of water and nanoparticles Jawad *et al.* [39]

Physical properties	Water base fluid	Cu	Fe_3O_4
ρ [kgm^{-3}]	997.1	8933	5200
c_p [Jkg^{-1}K^{-1}]	4179	385	670
k [Wm^{-1}K^{-1}]	0.613	401	6
$B\cdot10^5$ [K^{-1}]	21	1.67	1.3
$\sigma\cdot10^{-6}$ [cm^{-1}]	$5.5\cdot10^{-12}$	59.6	0.025

Non-dimensionalizing utilizing the following non-similarity transformation:

$$\eta = \sqrt{\frac{2\tilde{a}}{\nu_f \xi}} z, \quad \xi = 1 - e^{-\tilde{a}t}, \quad u(x,z,t) = \tilde{a}xF'(\xi,\eta), \quad v(x,z,t) = \Omega x V(\xi,\eta)$$

$$w(x,z,t) = -\sqrt{2\tilde{a}\nu_f \xi} F(\xi,\eta), \quad \theta = \frac{T - T_\infty}{T_w - T_\infty}, \quad \phi_1 = \frac{a}{a_0}, \quad \phi_2 = \frac{b}{a_0} \tag{16}$$

Substituting eq. (16) into eqs. (3)-(8), consequently continuity eq. (3) is automatically satisfied and the following non-dimensional flow governing equations are resulted:

$$\frac{2\mu_{\mathrm{nf}}}{\mu_{\mathrm{f}}}F'''+\frac{\rho_{\mathrm{nf}}}{\rho_{\mathrm{f}}}\left[2\xi FF''+\frac{1}{2}\eta(1-\xi)F''+\xi(1-F'^2+\lambda V^2)\right]+ \\ +\frac{\sigma_{\mathrm{nf}}}{\sigma_{\mathrm{f}}}\xi M_g(1-F')+\frac{(\rho\beta)_{\mathrm{nf}}}{(\rho\beta)_{\mathrm{f}}}\xi\gamma\theta=\frac{\rho_{\mathrm{nf}}}{\rho_{\mathrm{f}}}\xi(1-\xi)\frac{\partial F'}{\partial\xi} \tag{17}$$

$$\frac{2\mu_{\mathrm{nf}}}{\mu_{\mathrm{f}}}V''+\frac{2\rho_{\mathrm{nf}}}{\rho_{\mathrm{f}}}\xi(FV'-F'V)+\frac{1}{2}\frac{\rho_{\mathrm{nf}}}{\rho_{\mathrm{f}}}\eta\ (1-\xi)V'-\frac{\sigma_{\mathrm{nf}}}{\sigma_{\mathrm{f}}}\xi M_g V=\frac{\rho_{\mathrm{nf}}}{\rho_{\mathrm{f}}}\xi(1-\xi)\frac{\partial V}{\partial\xi} \tag{18}$$

$$\frac{2k_{\mathrm{nf}}}{k_{\mathrm{f}}}\frac{1}{\mathrm{Pr}}\theta''+\frac{(\rho c_p)_{\mathrm{nf}}}{(\rho c_p)_{\mathrm{f}}}\left[\frac{1}{2}\eta(1-\xi)\theta'+2\xi F\theta'\right]+\xi\delta\theta=\frac{(\rho c_p)_{\mathrm{nf}}}{(\rho c_p)_{\mathrm{f}}}\xi(1-\xi)\frac{\partial\theta}{\partial\xi} \tag{19}$$

$$\frac{2}{\mathrm{Sc}}\phi_1''+2\xi F\phi_1'+\frac{1}{2}\eta(1-\xi)\phi_1'-\xi K_c\phi_1\phi_2^2=\xi(1-\xi)\frac{\partial\phi_1}{\partial\xi} \tag{20}$$

$$\frac{2\delta^*}{\mathrm{Sc}}\phi_2''+2\xi F\phi_2'+\frac{1}{2}\eta(1-\xi)\phi_2'+\xi K_c\phi_1\phi_2^2=\xi(1-\xi)\frac{\partial\phi_2}{\partial\xi} \tag{21}$$

Associated with relevant boundary conditions:

$$F(\xi,0)=F'(\xi,0)=0,\quad V(\xi,0)=1,\quad \theta'(\xi,0)=\mathrm{Bi}[\theta(\xi,0)-1]$$

$$\phi_1'(\xi,0)=K_s\phi_1(\xi,0),\quad \delta^*\phi_2'(\xi,0)=-K_s\phi_1(\xi,0)$$

$$F'(\xi,\infty)\to 1,\quad V(\xi,\infty)\to 0,\quad \theta(\xi,\infty)\to 0,\quad \phi_1(\xi,\infty)\to 1,\quad \phi_2(\xi,\infty)\to 0 \tag{22}$$

Follow the particular case, assume that the diffusion coefficients D_A, D_B of reactants A and B are of same size (*i. e.* δ^*) according to Merkin [8]. hence due to this assumption the following expression has been gained:

$$\phi_1(\xi,\eta)+\phi_2(\xi,\eta)=1 \tag{23}$$

Consequently, eqs. (20) and (21) are simplified to be one equation:

$$\frac{1}{\mathrm{Sc}}\phi''+\xi FS'+\frac{1}{4}\eta(1-\xi)\phi'-\frac{1}{2}\xi K_c S(1-\phi)^2=\frac{1}{2}\xi(1-\xi)\frac{\partial\phi}{\partial\xi} \tag{24}$$

and conditions in eq. (22) becomes:

$$\phi'(\xi,0)=K_s\phi(\xi,0),\qquad \phi(\xi,\infty)\to 1 \tag{25}$$

The following important parameters are obtained, $M_g=(\sigma_{\mathrm{f}}B_0^2)/(\tilde{a}\rho_{\mathrm{f}})$ gives magnetic field parameter, $\lambda=(\Omega/\tilde{a})^2$ symbolizes the rotation parameter, γ = $\mathrm{Gr}/\mathrm{Re}^2$ means mixed convection parameter, $\mathrm{Gr}=[g\beta_{\mathrm{f}}(T_w-T_\infty)r^3]/\nu_{\mathrm{f}}^2$ refers to Grashof number, $\mathrm{Re}=Ux/\nu_{\mathrm{f}}$ represents Reynolds number, $K_c=(k_c a_0^2)/\tilde{a},$; $K_s=(k_s/D_A)[(\nu_{\mathrm{f}}\xi)/(2\tilde{a})]^{1/2}$ point out homogeneous and heterogeneous reaction strength, respectively, $\delta=Q_0/[\tilde{a}(\rho c_p)_{\mathrm{f}}]$ is heat generation or absorption parameter, δ^* = D_B/D_A gives the ratio of diffusion coefficients; $\mathrm{Pr}=[\mu_{\mathrm{f}}(c_P)_{\mathrm{f}}]/k_{\mathrm{f}}$ and $\mathrm{Sc}=\nu_{\mathrm{f}}/D_A$ stand for Prandtl and Schmidt numbers, remember that the prime sign "'" refers to differentiation with respect to the non-similarity variable, η.

The x– and y-direction shear stresses, respectively, are given by:

$$\mathrm{Re}^{1/2}\,\xi^{1/2}C_{fx}=\frac{2\mu_{\mathrm{nf}}}{\rho_{\mathrm{f}}U^2}\left(\frac{\partial u}{\partial z}\right)_{z=0}=2\sqrt{2}\,\frac{\mu_{\mathrm{nf}}}{\mu_{\mathrm{f}}}F''(\xi,0) \tag{26}$$

$$\mathrm{Re}^{1/2}\,\xi^{1/2}C_{fy}=-\frac{2\mu_{\mathrm{nf}}}{\rho_{\mathrm{f}}U^2}\left(\frac{\partial v}{\partial z}\right)_{z=0}=-2\sqrt{2}\lambda^{1/2}V'(\xi,0) \tag{27}$$

The rate of surface heat transfer in terms of Nusselt number is described by:

$$\mathrm{Re}^{-1/2}\,\xi^{1/2}\,\mathrm{Nu}=-\frac{k_{\mathrm{nf}}x}{k_{\mathrm{f}}(T_{\mathrm{w}}-T_{\infty})}\left(\frac{\partial T}{\partial z}\right)_{z=0}=-\sqrt{2}\,\frac{k_{\mathrm{nf}}}{k_{\mathrm{f}}}\theta'(\xi,0) \tag{28}$$

Thus, we have to tackle numerically eqs. (17)-(19), and (24) along with the boundary conditions (22) and (25) for some values of the resulting parameters.

Results and discussion

The combined aspects of homogeneous and heterogeneous reactions, unsteady mixed convection, convective boundary condition, internal heat generation or absorption and magnetic field on the flow of a viscous, incompressible, and electrically conducting nanofluid in a stagnation point of an impulsively rotating sphere is addressed. The nanofluid is water based fluid with a suspended nanoparticles of ferro, Fe_3O_4, and copper, Cu. The resulting non-linear partial differential equations along with the boundary conditions are tackled numerically *via* MATLAB routine bvp4c. Once again for establishing the validity of present results, these are compared with the computations in the literature. Figure 2 stands for a comparison of the values of $-V'(\xi, 0)$ with the data given by Takhar *et al.* [34] for various values of magnetic field parameter, M_g, and mixed convection parameter, γ. An excellent agreement is shown with our presented results.

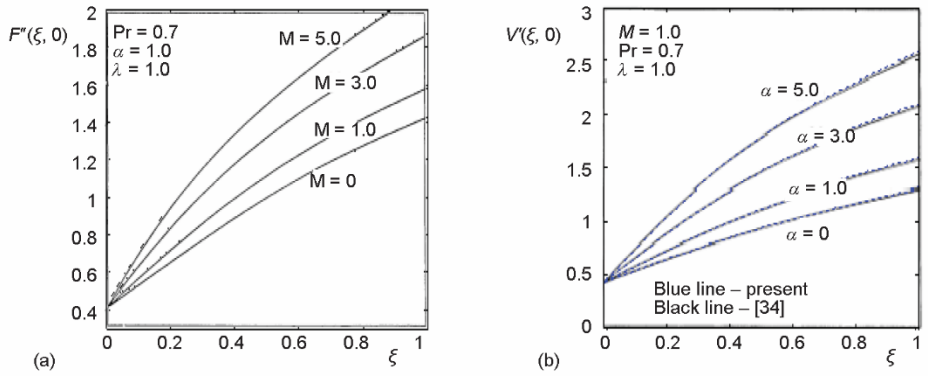

Figure 2. Comparison of the present results with those given by Takhar *et al.* [34] for $V'(\xi, 0)$ against (a) magnetic field, (2) mixed convection parameters

Once again, for highlighting the impacts of various significant parameters on x velocity, $F'(\xi, 0)$, temperature, $\theta(\xi, 0)$, and concentration, $\phi(\xi, 0)$, distributions for different suspended solid nanoparticle, here the graphical results are disclosed. The difference in species

concentration outline, $\phi(\xi, 0)$, for the measure of homogeneous K_c = 0.1, 0.5, 1, 2, and 10, and heterogeneous K_s = 0.1, 0.3, 0.5, 0.7, 1, 2, and 5, reactions strengths are presented in fig. 3. Aspects of K_c on the concentration distribution are displayed in fig. 3. It is noticed that with ascending the measure of homogeneous reaction strength the species concentration field decreases. Figure 3 as well demonstrates the influences of K_s on concentration curves $\phi(\xi, \eta)$. A reduction in concentration field is given when the measure of the strength of heterogeneous reaction K_s becomes higher. Figure 4 portrays that the species concentration at the sphere surface decays asymptotically when K_c and K_s approaches to infinity. Unlike, the characteristic of Schmidt number, Sc = 0.2, 0.44, 0.9, 1.3, and 2, leads to improve the species concentration distribution.

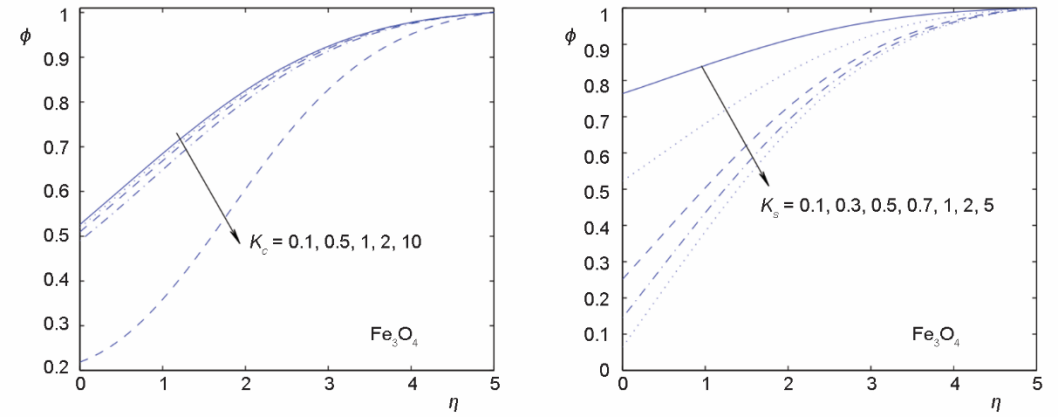

Figure 3. Impact of homogeneous and heterogeneous parameters on ϕ

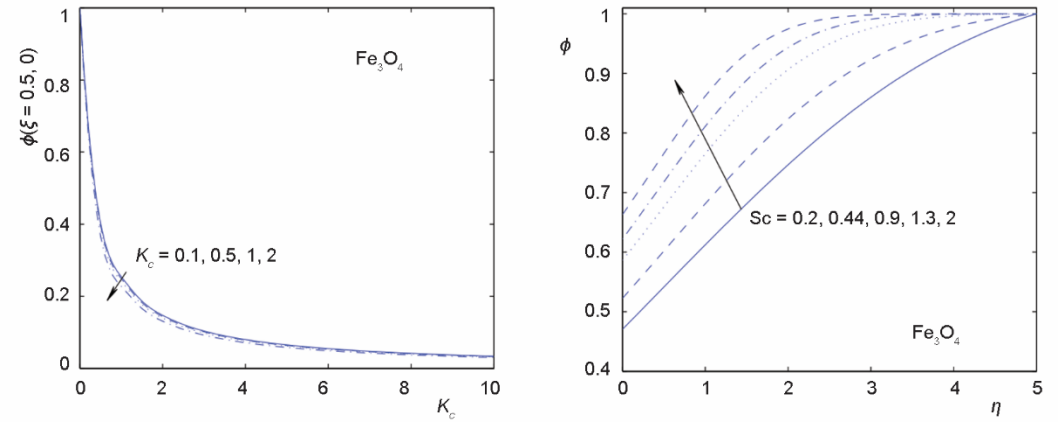

Figure 4. Impact of K_c and Sc parameters on ϕ

The influence of rotation parameter, λ = 1, 5, 10, 15, 20, and 25 on the x and y velocities, nanofluid temperature distributions, the rate of heat transfer and x and y shear stresses with Cu and Fe_3O_4 nanoparticles φ = 0.04 is stated in figs. 5-7. An enhance in the rotation parameter, λ, posses strong positive impacts on the rate of heat transfer and shear stresses. All of Nu(ξ, 0), $F''(\xi, 0)$, and $V'(\xi, 0)$ boost with rising values of rotation parameter, λ. Besides, the

y velocity and nanofluid temperature fields reduce, slightly, with ascending the rotation parameter. Because of the reduction of momentum and thermal boundary-layers which leads to augment the velocity and temperature gradients at the wall. Again the nanofluid velocity, F', becomes larger with higher values of λ. Figures 8 and 9 are provided to analyze the aspects of Biot number, Bi = 0.1, 0.5, 1, 5, 10, and ∞, and solid volume fraction of nanoparticles φ = 0.0, 0.02, 0.03, 0.04, and 0.10, with Cu and Fe_3O_4 suspended nanoparticles on the nanofluid temperature distributions and rate of heat transfer. Clearly, as both Bi and φ rise, the rate of heat transfer, nanofluid temperature field $\theta(\xi, \eta)$ and thermal boundary-layer thickness enhance. Therefore, adding of nanoparticles in the base fluid is responsible for the enhancement in thermal conductivity of the fluid.

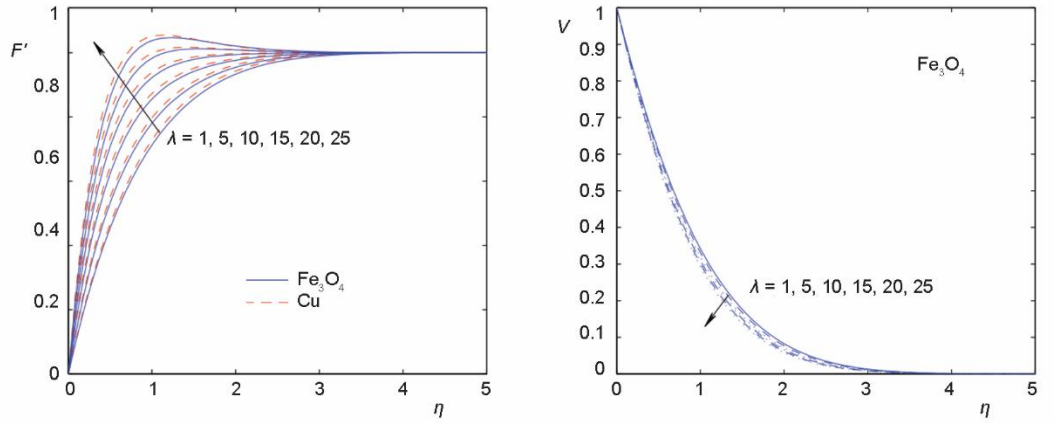

Figure 5. Impact of λ parameter on *x* and *y* velocity components

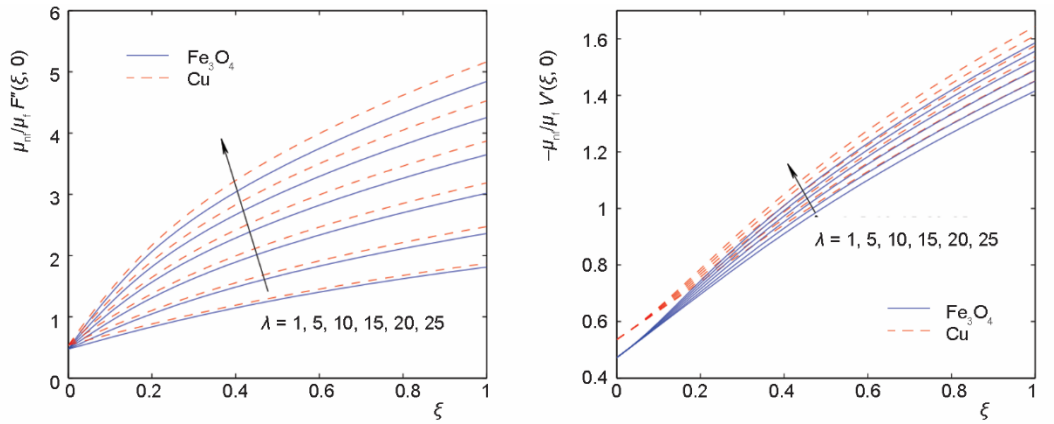

Figure 6. Impact of λ parameter on *x* and *y* components of shear stress

The impact of heat generation parameter, δ = –1.0, 0.5, –0.1, 0, 0.1, and 0.5, on the temperature profile and local Nusselt number is elucidated in fig. 10. With rising values of heat generation parameter, δ, the nanofluid temperature augments. This result is as per the expectations because any heat generated would cause an upgrade in the thermal energy of the nanofluid. The augment in nanofluid temperature has susceptibility to rise the thermal buoyancy

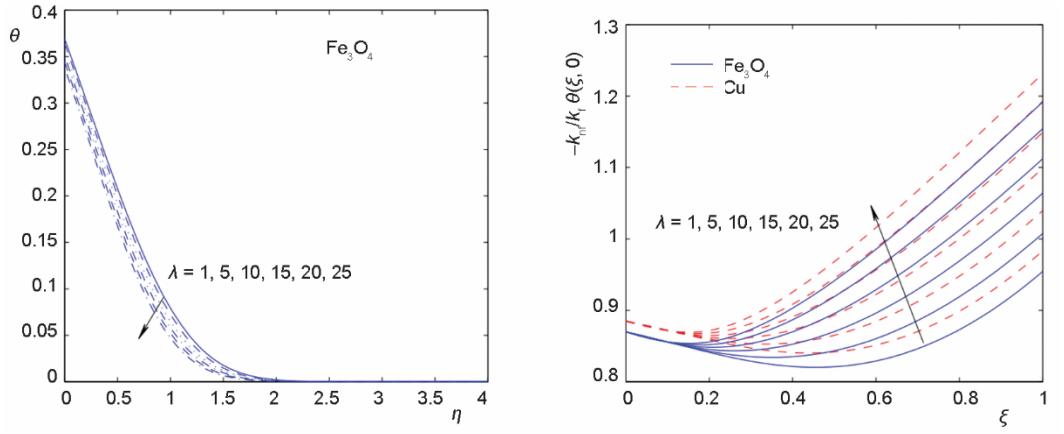

Figure 7. Impact of λ parameter on θ and Nu profiles

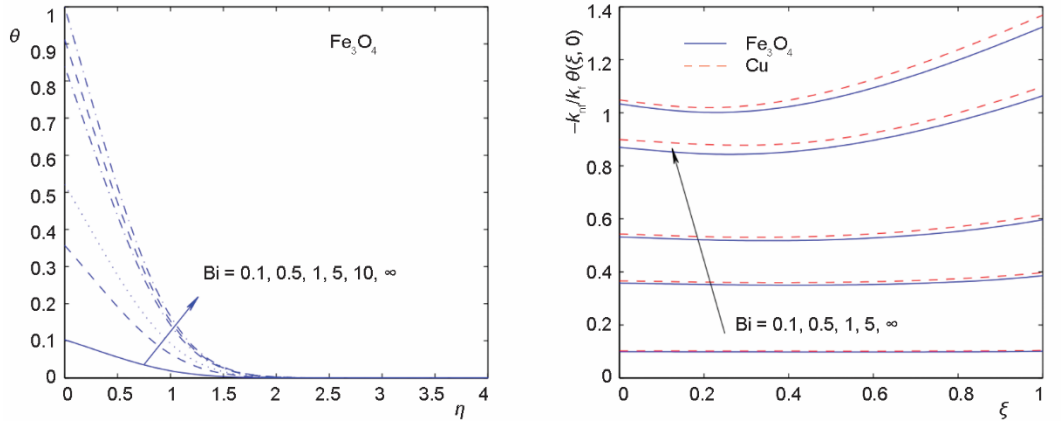

Figure 8. Impact of Biot number on θ and Nu profiles

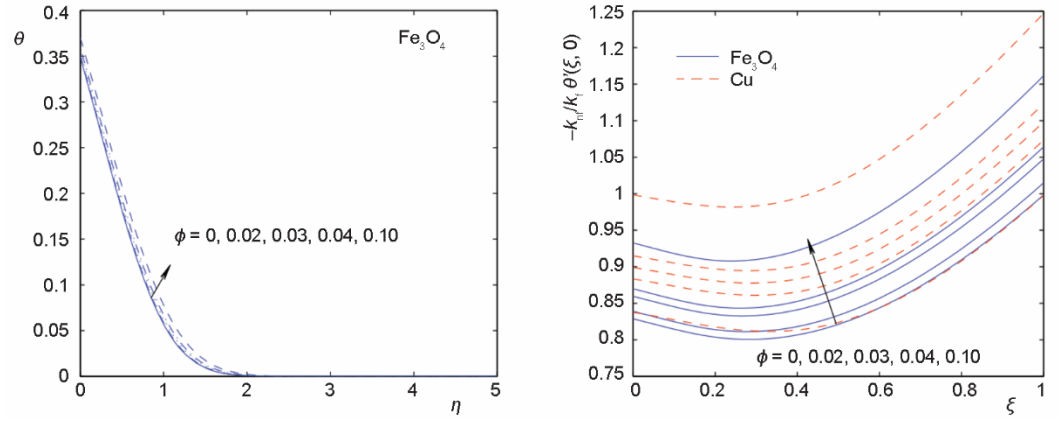

Figure 9. Aspects of Ec parameter on θ and Nu profiles

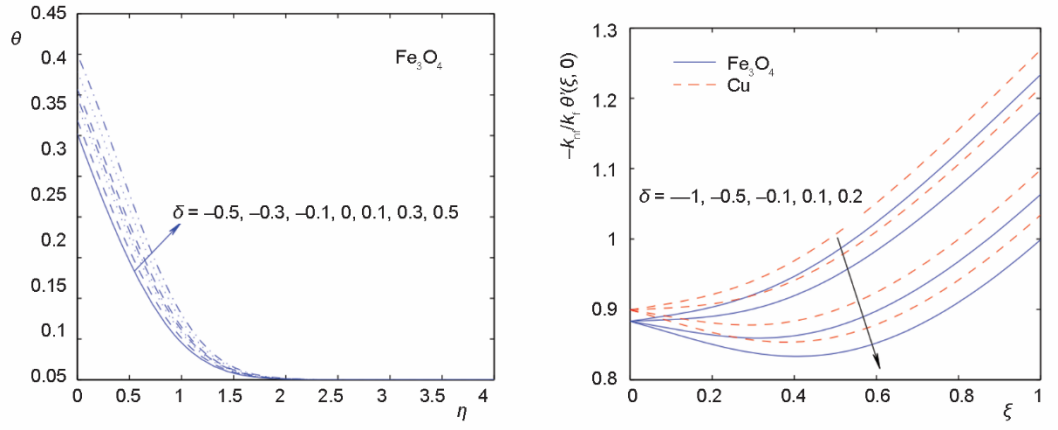

Figure 10. Impact of δ parameter on θ and Nu profiles

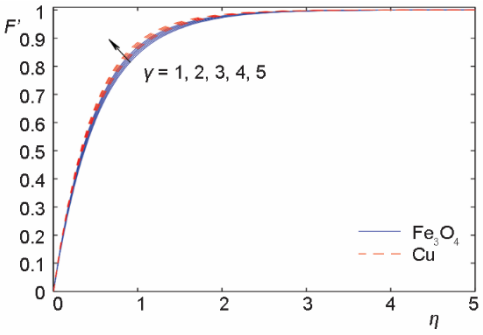

Figure 11. Impact of γ parameter on F' profiles

force. This gives higher buoyancy induced flow along the sphere surface. Moreover rising values of heat generation parameter leads to reduce the rate of heat transfer as given in terms of local Nusselt number. The difference in temperature profile θ, Nusselt number, Nu(ξ, 0), velocity profile F', and x and y shear stresses *i. e.* $F''(\xi, 0)$, $V'(\xi, 0)$ with Cu and Fe_3O_4 nanoparticle, against ξ for some various values of mixed convection parameter, γ = 1, 2, 3, 4, and 5, are produced in figs. 11-13. From illustrated figures Nu(ξ, 0), $F''(\xi, 0)$, and $V'(\xi, 0)$ augment as the mixed convection parameter, γ, rises this caused by descent of viscous and thermal boundary-layer thicknesses. Since the positive buoyancy force affects such a affirmative pressure gradient which makes the fluid motion accelerated inside the boundary-layer. Consequently descent the thickness of thermal and momentum boundary-layers and this in turn enlarge the shear stresses and heat transfer rate at the surface.

Figure 14 gives the influence of magnetic field parameter M_g = 0, 0.1, 0.5, 1, 2, and 5, on x and y velocity component. Clearly magnetic field parameter reduces velocity components outlines. With the physical estimation, the currently phenomena is found as the magnetic field provides current in the conductive fluid, then it gives a resistive-type force (known as Lorentz force) on the fluid inside boundary-layer, which diminishes the fluid activity. This deficiency of the velocity distributions increases both of the velocity and thermal boundary-layer thicknesses which upgrades the Nu(ξ, 0), $F''(\xi, 0)$, and $V'(\xi, 0)$. The surface shear stresses and rate of heat transfer are independent of magnetic field M_g as ξ = 0 (at the motion start), after that the aspect of M_g rises with ξ.

Conclusions

The impacts of unsteady mixed homogeneous and heterogeneous reactions, internal heat generation, convective boundary condition and magnetic field on a viscous flow, incompressible, and electrically conducting nanofluid in stagnation-point of rotating sphere was

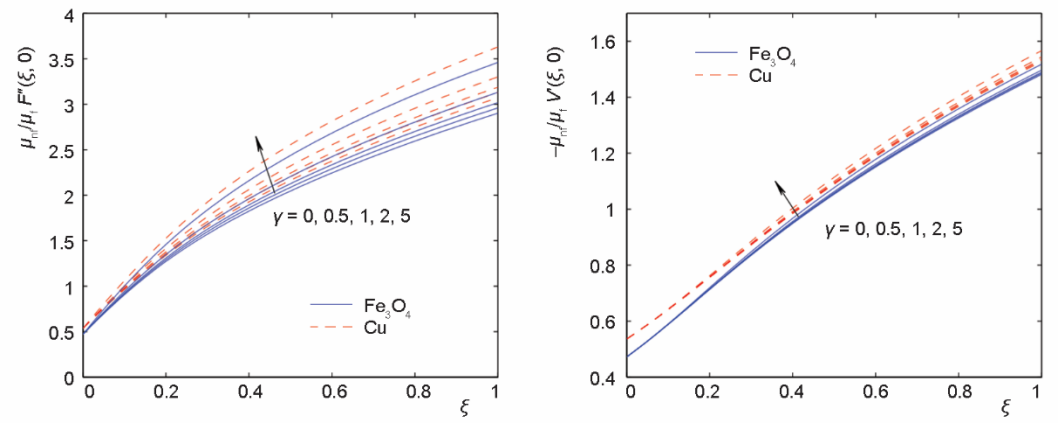

Figure 12. Impact of γ parameter on x and y components of shear stress

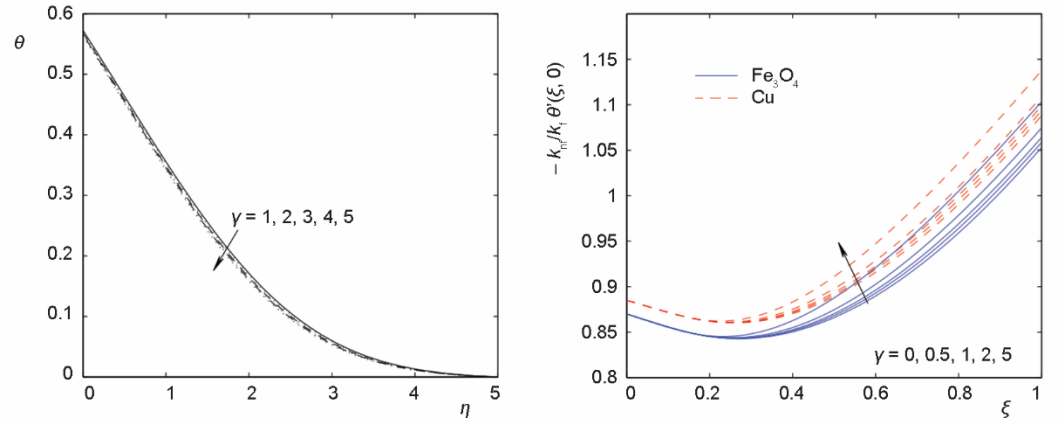

Figure 13. Impact of γ parameter on θ and Nu profiles

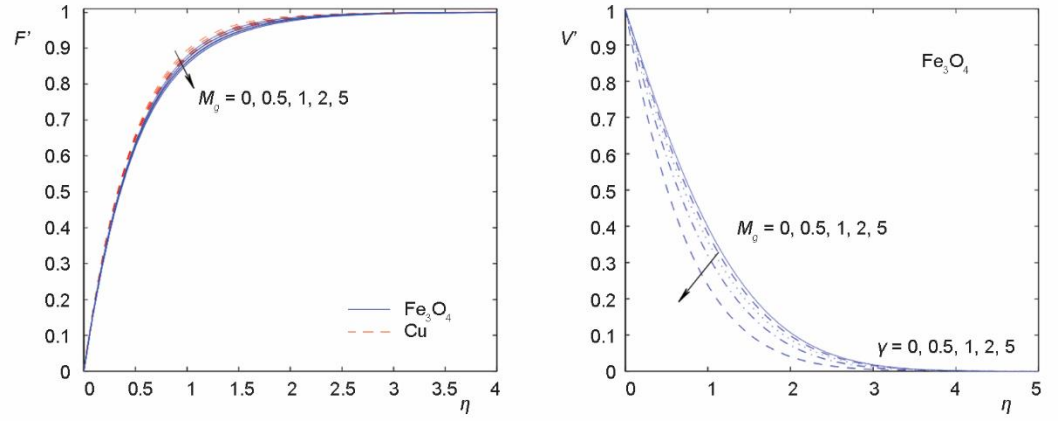

Figure 14. Impact of M_g parameter on x and y components of velocity

inspected. The problem was modeled due to Navier stokes equations with Boussinesq approximation and then the resulting governing flow equations have been treated numerically via the MATLAB routine bvp4c. We have illustrated, inter alia, an augment in the nanoparticle solid volume fraction leads to rise the species concentration and nanofluid velocity in the case of a Fe_3O_4-water nanofluid whereas it has an opposite impact on species concentration and nanofluid velocity in the case of a Au-water nanofluid. An increment in the volume fraction of the nanoparticles rises the nanofluid temperature. Internal heat generation parameter causes an augment in the nanofluid temperature. The species concentration is reduced by ascending in the homogeneous and heterogeneous reaction strength and the concentration at the sphere surface approaches zero as the homogeneous and heterogeneous reaction rate becomes higher. that the impact of the magnetic field parameter is to diminish the species concentration and the flow but boost the nanofluid temperature.

Nomenclature

A – unsteadiness parameter
a, b – concentrations of chemical species
B_0 – strength of magnetic field, [T]
c_p – specific heat, [$Jkg^{-1}K^{-1}$]
D_A – diffusion coefficient of chemical spicie a
D_B – diffusion coefficient of chemical spicie b
Ec – Eckert number
F – non-dimensional stream function
k – thermal conductivity, [$Wm^{-1}K^{-1}$]
K_c – homogeneous reaction parameter
K_s – heterogeneous reaction parameter
K^* – permeability
M_g – magnetic field parameter
Nu – nusselt number
Pr – prandtl number
Re – reynolds number
Sc – schmidt number
T – dimensional temperature, [K]
t – time, [s]
(u, v) – velocity components, [ms^{-1}]
(x, y) – cartesian co-ordinates, [m]

Greek symbols

γ – constant, [s^{-1}]
δ – ratio of diffusion coefficients
θ – dimensionless temperature
μ – dynamic viscosity, [$kgm^{-1}s^{-1}$]
ν – kinematic viscosity, [m^2s^{-1}]
ρ – fluid density, [kgm^{-3}]
σ – electrical conductivity, [$Wm^{-1}K^{-1}$]
φ – nanoparticles solid volume fraction

Subscripts

∞ – conditions in the free stream
f – fluid
nf – nanofluid particle
p – solid material
w – conditions at the surface

References

[1] Song, X., *et al.* Steady States and Oscillations in Homogeneous-Heterogeneous Reactions Systems, *Chem. Eng. Sci., 46* (1991), 5-6, pp. 1203-1215
[2] Song, X., *et al.*, The Ignition Criteria for Stagnation-Point Flow: SemenovFrank Kamenetskii or van't Hoff, *Combust. Sci. and Tech., 75* (1991), 4-6, pp. 311-331
[3] Song, X., *et al.* Bifurcation Behaviour in Homogeneous-Heterogeneous Combustion. II. Computations for Stagnation-Point Flow, *Combust Flame, 84* (1991), 3-4, pp. 292-311
[4] Williams, W. R., *et al.*, Ignition and Extinction of Surface and Homogeneous Oxidation of NH_3 and CH_4. *AIChE J., 37* (1991), 5, pp. 641-649
[5] Williams, W. R., *et al.*, Bifurcation Behaviour in Homogeneous-Heterogeneous Combustion. I. Experimental Results over Platinum, *Combust. Flame, 84* (1991), 3-4, pp. 277-291
[6] Chaudhary, M. A., Merkin, J. H., A Simple Isothermal Model for Homogeneous-Heterogeneous Reactions in Boundary-Layer Flow. II Unequal Diffusivities, *Fluid Dyn. Res., 16* (1995), 6, pp. 335-359
[7] Chaudhary, M. A., Merkin, J. H., A Simple Isothermal Model for Homogeneous-Heterogeneous Reactions in Boundary-Layer Flow. I Equal Diffusivities, *Fluid Dyn. Res., 16* (1995), 6, pp. 311-333
[8] Merkin, J. H., A Model for Isothermal Homogeneous-Heterogeneous Reactions in Boundary-layer Flow, *Math. Comput. Model., 24* (1996), 8, pp. 125-136
[9] Hayat, T., *et al*., Stagnation Point Flow with Cattaneo-Christov Heat Flux and Homogeneous-Heterogeneous Reactions, *J. Mol. Liq., 220* (2016), Aug., pp. 49-55

[10] Khan, W. A., Pop, I., Effects of Homogeneous-Heterogeneous Reactions on the Viscoelastic Fluid towards a Stretching Sheet, *ASME J. Heat Trans., 134* (2012), 6, ID 064506
[11] Khan, M. I., *et al*., Impact of Heat Generation/Absorption and Homogeneous-Heterogeneous Reactions on Flow of Maxwell Fluid, *J. Mol. Liq., 233* (2017), May, pp. 465-470
[12] Hayat, T., *et al*., Similarity Transformation Approach for Ferromagnetic Mixed Convection Flow in the Presence of Chemically Reactive Magnetic Dipole, *AIP Phys. Fluid., 28* (2016), 10, ID 102003
[13] Ashorynejad, H. R., *et al.*, Nanofluid Flow and Heat Transfer due to a Stretching Cylinder in the Presence of Magnetic Field, *Heat Mass Transf., 49* (2013), Dec., pp. 427-436
[14] Abu-Nada, E., *et al*., Natural Convection Heat Transfer Enhancement in Horizontal Concentric Annuli Using Nanofluids, *Int. Commun. Heat Mass Transf., 35* (2008), 5, pp. 657-665
[15] Tiwari, R. K., Das, M. K., Heat Transfer Augmentation in a Two-Sided Lid-Driven Differentially Heated Square Cavity Utilizing Nanofluids, *Int. J. Heat Mass Transfer, 50* (2007), 9-10, pp. 2002-2018
[16] Buongiorno, J. Convective Transport in Nanofluids, *ASME J. Heat Transfer, 128* (2006), 3, pp. 240-250
[17] Mahdy, A., Unsteady Mixed Convection Boundary-layer Flow and Heat Transfer of Nanofluids due to Stretching Sheet, *Nucl. Eng. Des., 249* (2012), Aug., pp. 248-255
[18] Choi, S. U. S., Eastman, J. A., Enhancing Thermal Conductivity of Fluids with Nanoparticles, *Proceedings,* ASME Int. Mech. Eng. Congress and Exposition, San Francisco, Cal., USA, 1995, pp. 99-105
[19] Mahdy, A., Sameh, E. A., Laminar Free Convection over a Vertical Wavy Surface Embedded in a Porous Medium Saturated with a Nano Fluid, *Transp. Porous Med., 91* (2012), Sept., pp. 423-435
[20] Mahdy, A., Entropy Generation of Tangent Hyperbolic Nano Fluid Flow past a Stretched Permeable Cylinder: Variable Wall Temperature, *Proc IMechE Part E: J Process Mechanical Engineering, 233* (2019), 3, pp. 570-580
[21] Mahdy, A., Chamkha, A. J., Unsteady MHD Boundary-layer Flow of Tangent Hyperbolic Two-Phase Nanofluid of Moving Stretched Porous Wedge, *International Journal of Numerical Methods for Heat and Fluid Flow, 28* (2018), 11, pp. 2567-2580
[22] Mahdy, A., Aspects of Homogeneous-Heterogeneous Reactions on Natural Convection Flow of Micropolar Fluid past a Permeable Cone, *Applied Mathematics and Computation, 352* (2019), July, pp. 59-67
[23] Oztop, H. F., Abu-Nada, E., Numerical Study of Natural Convection in Partially Heated Rectangular Enclosures Filled with Nanofluids, *Int. J. Heat Fluid Flow, 29* (2008), 5, pp. 1326-1336
[24] Mahdy, A., Simultaneous Impacts of MHD and Variable Wall Temperature on Transient Mixed Casson Nanofluid Flow in the Stagnation Point of Rotating Sphere, *Appl. Math. Mech. Engl. Ed., 39* (2018), May, pp. 1327-1340
[25] Chaudhary, M. A., Merkin, J. H., A Simple Isothermal Model for Homogeneous-Heterogeneous Reactions in Boundary-layer Flow: I. Equal Diffusivities, *Fluid Dynam. Res., 16* (1995), 6, pp. 311-333
[26] Mahdy, A., Ahmed, S. E., Unsteady MHD Convective Flow of Non-Newtonian Casson Fluid in the Stagnation Region of an Impulsively Rotating Sphere, *J. Aer. Engin., 30* (2017), 5, ID 04017036
[27] Sameh, E. A., Mahdy, A., Unsteady MHD Double Diffusive Convection in the Stagnation Region of an Impulsively Rotating Sphere in the Presence of Thermal Radiation Effect, *J. Taiwan Institute Chem. Engn., 58* (2016), Jan., pp. 173-180
[28] Mahdy, A., Chamkha, A. J., Heat Transfer and Fluid Flow of a Non-Newtonian Nanofluid over an Unsteady Contracting Cylinder Employing Buongiorno's Model, *International Journal of Numerical Methods and Heat Fluid Flow, 25* (2015), 4, pp. 703-723
[29] Nor, A. M. Z., *et al*., Analysis of Heat Transfer for Unsteady MHD Free Convection Flow of Rotating Jeffrey Nanofluid Saturated in a Porous Medium, *Res. Phys., 7* (2017), Dec., pp. 288-309
[30] Abid, H., *et al*., Convection Heat Transfer in Micropolar Nanofluids with Oxide Nanoparticles in Water, Kerosene and Engine Oil, *J. Mol. Liq., 229* (2017), Mar., pp. 482-488
[31] Jawad, R., *et al*., Magnetohydrodynamic Flow of Molybdenum Disulfide Nanofluid in a Channel with Shape Effects, *Multidiscipline Modeling in Materials and Structures, 15* (2019), 4, pp. 737-757
[32] Liaquat, A. L., *et al*., Stability Analysis of Darcy-Forchheimer Flow of Casson Type Nanofluid Over an Exponential Sheet: Investigation of Critical Points, *Symmetry, 11* (2019), 3, ID 412
[33] Chamkha, A. J., *et al*., Unsteady MHD Rotating Flow over a Rotating Sphere near the Equator, *Acta Mechanica, 164* (2003), 1-2, pp. 31-46
[34] Takhar, H. S., *et al*., Unsteady Free Convection Flow in the Stagnation-Point Region of a Rotating Sphere, *International Journal Non-Linear Mechanics, 33* (1998), 5, pp. 857-865

[35] Takhar, H. S., *et al.*, Unsteady Laminar MHD Flow and Heat Transfer in the Stagnation Region of an Impulsively Spinning and Translating Sphere in the Presence of Buoyancy Forces, *Heat and Mass Transfer, 37* (2001), July, pp. 397-402
[36] Ikeda, H., *et al*., Catalytic Combustion of Hydrogen-Air Mixtures in Stagnation Flows, *Combust Flame, 93* (1993), 1-2, pp. 138-148
[37] Brinkman, H. C., The Viscosity of Concentrated Suspensions and Solution, *J. Chem. Phys., 20* (1952), 4, pp. 571-581
[38] Jawad, R., *et al*., Numerical Investigation of Copper-Water (Cu-Water) Nanofluid with Different Shapes of Nanoparticles in a Channel with Stretching Wall: Slip Effects, *Math. Comput. Appl., 21* (2016), 4, pp. 43-58
[39] Maxwell, J., *A Treatise on Electricity and Magnetism*, 2nd ed. Oxford University Press, Cambridge, UK, 1904

Paper submitted: July 12, 2019
Paper revised: July 30, 2019
Paper accepted: August 7, 2019